Threshold of coexistence and critical behavior of a predator-prey stochastic model in a fractal landscape

View the table of contents for this issue, or go to the journal homepage for more

You may also be interested in:

Critical behavior of the absorbing transition of branching and annihilating bosonic random walkers
C Argolo, Pedro H Barros, Iram Gleria et al.

The threshold of coexistence and critical behaviour of a predator--prey cellular automaton
Everaldo Arashiro and Tânia Tomé

Two competitive contact processes with local interactions
T B Pedro, M M Szortyka and W Figueiredo

Non-equilibrium critical behaviour on fractal lattices
I Jensen

Non-equilibrium relaxation in a stochastic lattice Lotka-Volterra model
Sheng Chen and Uwe C Täuber

Conserved directed percolation: exact quasistationary distribution of small systems andMonte Carlo simulations
Júlio César Mansur Filho and Ronald Dickman

Stable oscillations of a predator--prey probabilistic cellular automaton
Tânia Tomé and Kelly C de Carvalho

Threshold of coexistence and critical behavior of a predator-prey stochastic model in a fractal landscape

C Argolo[1,2], P Barros[3], T Tomé[4], E Arashiro[5], Iram Gleria[6] and M L Lyra[6]

[1] Núcleo de Ciências Exatas - NCex, Universidade Federal de Alagoas, 57309-005 Arapiraca-AL, Brazil
[2] On leave of Instituto Federal de Ciência e Tecnologia do Estado de Alagoas, 57020-510 Maceió-AL, Brazil
[3] Instituto Federal de Ciência e Tecnologia do Estado de Alagoas, 57020-510 Maceió-AL, Brazil
[4] Instituto de Física, Universidade de São Paulo, 05315-970 São Paulo, SP, Brazil
[5] Instituto de Matemática, Física e Estatística, Universidade Federal do Rio Grande, 96201-900 Rio Grande, RG, Brazil
[6] Instituto de Física, Universidade Federal de Alagoas, 57072-970 Maceió AL, Brazil
E-mail: iram@fis.ufal.br and iram@pq.cnpq.br

Abstract. We investigate a stochastic lattice model describing a predator-prey system in a fractal scale-free landscape, mimicked by the fractal Sierpinski carpet. We determine the threshold of species coexistence, that is, the critical phase boundary related to the transition between an active state, where both species coexist and an absorbing state where one of the species is extinct. We show that the predators must live longer in order to persist in a fractal habitat. We further performed a finite-size scaling analysis in the vicinity of the absorbing-state phase transition to compute a set of stationary and dynamical critical exponents. Our results indicate that the transition belongs to the directed percolation universality class exhibited by the usual contact process model on the same fractal landscape.

Keywords: absorbing states, critical exponents and amplitudes

Contents

1. Introduction

Stochastic spatial structured models have been largely used to describe biological population problems [1–18]. Unlike continuous models of ordinary differential equations based on the law of mass action, stochastic lattice models take into account the discreteness of individuals [3, 19]. Also, stochastic local interactions play an important role in population cycles [18, 20–22]. In particular, a probabilistic cellular automata model of a predator-prey system has been introduced to determine the threshold of species coexistence in a two dimensional regular lattice [11, 14, 23]. The possible influence of the lattice topology on the population dynamics has driven a lot of interest in the recent literature. One of the motivations was the pioneering experimental study carried out by Huffaker, who showed that persistence of a given species demands non-homogeneous space [25]. In the case of low population sizes, or populations dispersed in heterogeneous habitats, probabilistic cellular automata and stochastic lattice models are appropriate and necessary to analyze the role of space in the coexistence of species (see [23] and references therein).

In this work, we will focus on the class of stochastic spatial structured models and consider the predator-prey system introduced in [4], which exhibits a phase diagram with active states where both species coexist and an absorbing state where one of the species has been extinct. This probabilistic cellular automata takes predator-prey interactions into account through a Lotka–Volterra type mechanism. Spectral densities and time correlation functions were presented in [18], where the authors analyzed coexistence and linked population cycles. Numerical studies have pointed out that the extinction transition presented by this model belongs to the directed percolation universality class [1, 23, 24]. Here, we will investigate the effect of landscape fractality on the dynamics of interacting populations by considering that the individuals are restricted to occupy the sites of a Sierpinski fractal carpet with fractal dimension $d_{\mathrm{f}} = \log 8/\log 3$. Since the translational symmetry is broken into fractals, one question is to understand how the scale invariance of the underlying self-similar landscape can affect the absorbing transition. Movement of organisms in complex

habitats is often assessed through the use of fractals [26]. Fractal habitats are used when considering habitat fragmentation, a process that produces isolated patches which are highly irregular [16]. For example, in [15] the effect on fractal fragmentation was considered and the authors found that fractal landscape allows for more degradation than predicted for regular ones. Also, studies of habitat structures at scales compatible to the species considered showed a relationship between fractal dimension and space convolution [17]. In the Sierpinski fractal, the forbidden sites (patches) correspond to the 'holes' in the fractal. We will unveil that the predators must live longer in order to persist in such fractal habitat. We also analyze the continuous second-order phase transition present in the model and locate it by means of the relative fluctuation (cumulant) technique. In order to find the critical properties, we perform Monte Carlo simulations and finite-size, as well as short-time, scaling analysis. In this way, we determine a set of critical exponents which allows the classification of the model's universality class. The estimated exponents are consistent with the ones of the directed percolation universality class in the fractal considered.

The paper is organized as follows: section 2 presents our model and the numerical procedure; in section 3 we present and discuss our main results; in section 4 we summarize and draw our conclusions.

2. Model and simulations

We study a stochastic and space structured model describing an ecological system of two species. For this purpose, we consider a lattice on which each allowed site can be in one of three possible states: occupied by a prey individual (X), an individual predator (Y) or an empty site (Z). Actually prey-like sites can also represent a site in which food is available for predators. The habitat where the individuals survive, interact and proliferate is supposed to be the fractal Sierpinski carpet. Our model takes into account the following reactions:

$$
\begin{aligned}
X + Z &\xrightarrow{a} 2X \\
X + Y &\xrightarrow{b} 2Y \\
Y &\xrightarrow{c} Z,
\end{aligned}
\tag{1}
$$

where a, (b) is the prey (predator) proliferation probability, and c is the predator death probability. We assume $a + b + c = 1$ and are constrained to $[0, 1]$. Our stochastic fractal lattice model is defined by an asynchronous global dynamics composed by the following set of Markovian rules:

(a) *Prey proliferation.* In an empty site, an individual prey can be born with a probability a/z times the number of sites occupied by prey in the closest neighborhood. The parameter a is related to prey proliferation and $z = 4$ is the coordination number of the lattice. Because of the fractal structure, it may have none, one, two, three or four (prey) neighbors depending on the position of the lattice;
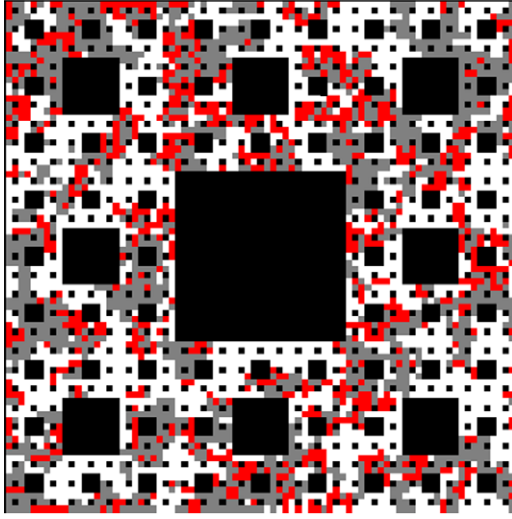
Figure 1. Configuration at $t = 600$ MCS for the predator-prey model on the Sierpinski fractal lattice with linear size $L = 3^4$ ($N = 8^4$ sites). The reaction rates are $a = 0.4$ and $b = 0.5$. Predators are in red, prey are in white and empty sites are in gray. Black holes are the forbidden sites of the Sierpinski fractal.

(b) *Predation, death of prey and birth of predators.* In a site occupied by a prey, an individual predator can be born with a probability $b/4$ times the number of sites occupied by predators in the closest neighborhood. Likewise with the prey, it may have none, one, two, three or four predator neighbors depending on the position of the lattice. In this process, there occurs an instantaneous prey death;

(c) *Death of predators.* Each predator dies spontaneously with probability c and leaves an empty site. This process reintegrates to the system the resources for prey proliferation.

It is appropriate to consider the critical behavior, characterized by a set of static critical exponents, obtained by the use of a finite-size scaling analysis of the critical order parameter and its relative fluctuations. In what follows, we show results from simulations on finite lattices with up to $N = 8^k$ sites (k is the generation number of the fractal). Each lattice sweep is considered as the time unit or one Monte Carlo step (MCS). The process is updated sequentially. Once the system is placed in the initial condition, we apply rules (a)–(c) above. The system evolves in time and eventually reaches a statistically stationary state (see figure 1 for a typical configuration during the system evolution).

We measured the order parameter, i.e. the density of predators:

$$\rho = \frac{\langle N_Y \rangle}{N}, \tag{2}$$

where N_Y is the number of predators in the stationary regime. The second moment of the order parameter is also computed in order to estimate a complete set of stationary critical exponents. The time evolution of the order parameter and its second moment at the absorbing transition is also followed to probe the critical dynamics.
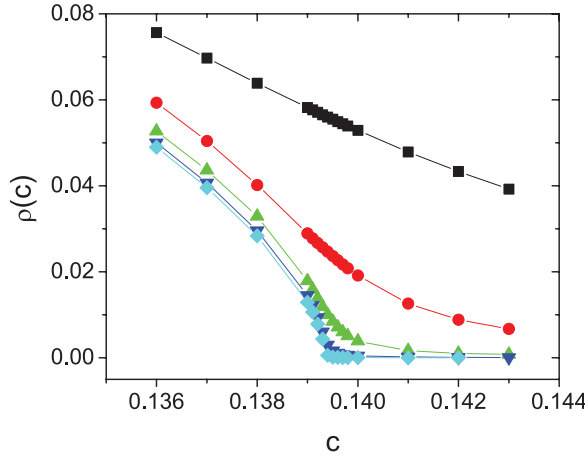
Figure 2. Statistically stationary density of predators $\rho(c)$ versus c for distinct k generations (different linear lattice sizes) of the Sierpinski carpet. From top to bottom $k = 3$, 4, 5, 6, and 7. A transition towards an absorbing state develops in the limit of large lattice sizes.

3. Results

In the following results related to the statistically stationary state, we performed calculations discarding the first L^2 runs (MCS) for a proper relaxation. We start from an initial condition with a single predator placed in a randomly chosen site of the fractal while the remaining site are occupied by prey. To avoid the absorbing state, we activate an individual predator in a randomly chosen site whenever the system becomes trapped in a state fully composed of prey, i.e. we assumed the prey absorbing and vacuum states as reflective boundaries. This approach has been successfully used in the literature and it is able to accurately account for the critical behavior of the absorbing-state phase transition after a proper finite-size scaling analysis [28–30]. Typical averages were performed over $n = 10^6$ distinct configurations for the smallest lattices up to $n = 10^3$ for the largest ones.

In figure 2 we show the average density of predators ρ as a function of the spontaneous death probability c, as obtained from simulations on lattices of distinct k generation and linear size $L = 3^k$. As $L \to \infty$ a transition from a state with nonzero density of predators to the prey absorbing state takes place by increasing the values of c. The values used in our simulations were $a = 0.4$ and $0.136 < c < 0.143$ with step 0.0001 near the critical point. To precisely locate the critical spontaneous death probability c_c, we measured the ratio between the second moment and squared first moment of the average predators number, defined as:

$$U_L(c) = \frac{\left\langle N_Y^2 \right\rangle}{\left\langle N_Y \right\rangle^2} \tag{3}$$

which is expected to be independent of the system size at the critical point and is related to the second order cumulant. In figure 3 we plot $U_L(c)$ obtained from simulations performed in distinct lattice sizes (different k generations), which allowed us to estimate the
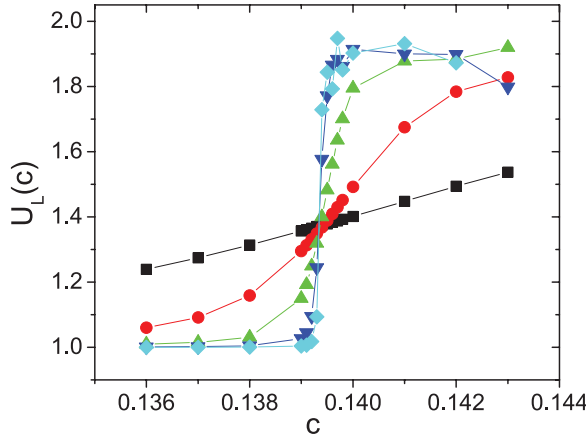
Figure 3. The moment ratio $U_L(c)$ as a function of the predators death probability c for distinct k generations (different lattice sizes). Same values of k as in figure 2. The scale invariance at the critical point allowed us to precisely estimate the critical predator spontaneous death probability $c_c = 0.139\,34(1)$.

critical probability as $c_c = 0.139\,34(1)$. It is important to stress that in a regular square lattice, the critical value of the predator death rate is $c_c = 0.188$ [1]. As expected, the fractal geometry difficult the coexistence of species and the survival of the predator population, implying that the predator species must live (on average) longer to persist in a fractal habitat. It is worth calling attention to the fact that a change of just 5% on the lattice dimensionality (from $d = 2$ on the square lattice to $d_f = \ln 8/\ln 3 = 1.89$ on the Sierpinski carpet) leads to a relatively large change (of the order of 25%) in the critical death rate, corresponding to *circa* 35% increase in the average lifetime.

The above result indicates that other topological measures, besides the fractal dimension, may play a relevant role in the critical death rate. Usually, the critical death rate is proportional to the lattice connectivity. In the Sierpinski carpet, the effective birth rate of predators is reduced, as compared to that in the regular square lattice, due to the smaller average number of neighbors. In the square lattice each site has four neighbors, except those on the border which can be neglected in large lattices. For the Sierpinski Carpet, the average number of neighbors per site in large lattices is $16/5 = 3.2$ [33]. Therefore such a smaller number of neighbors would account for a reduction of $3.2/4 = 20\%$ in the critical death rate. Our result points that both the reduction in dimensionality and local connectivity are thus relevant for the observed change in the critical point.

Having once located the critical point, finite-size scaling relations were used to compute the critical exponents characterizing such non-equilibrium phase transition. In particular, the order-parameter at the critical point obeys the power-law $\rho(c) \propto L^{-\beta/\nu_\perp}$, while its logarithmic derivative scales as $\frac{\mathrm{d}\log\rho(c)}{\mathrm{d}c} \propto L^{1/\nu_\perp}$. These scaling laws are depicted in figures 4 and 5 from which we estimate $\beta/\nu_\perp = 0.72(3)$ and $\nu_\perp = 0.79(2)$ for the fractal lattice. In order to estimate an additional stationary critical exponent, we calculate the order parameter fluctuations:
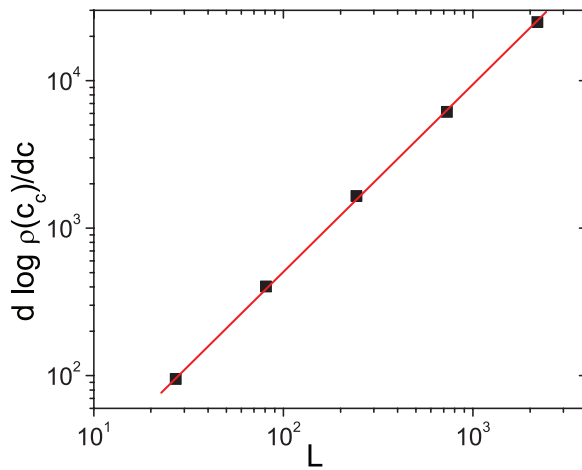
$$\Delta\rho(c) = \left[\left\langle N_Y^2 \right\rangle - \left\langle N_Y \right\rangle^2\right] N, \tag{4}$$
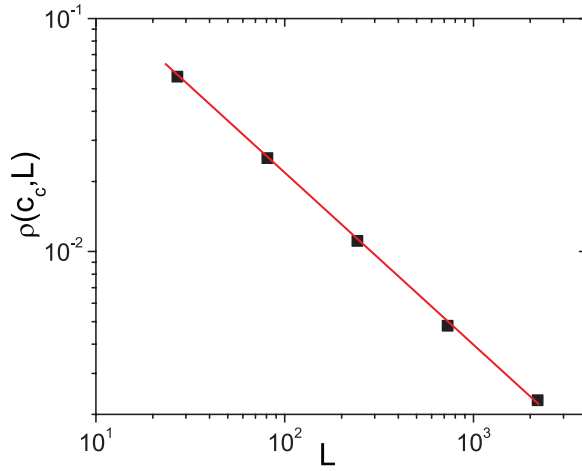
Figure 4. Log–log plot of the order parameter versus the linear size L. From the best fit to a power-law we estimate the critical exponent ratio $\beta/\nu_\perp = 0.72(3)$. For the square lattice this exponent is $\beta/\nu_\perp = 0.796(2)$.


Figure 5. The logarithmic derivative of the critical order parameter versus L (in log–log scale). From the best fit to a power-law we estimate the critical exponent $\nu_\perp = 0.79(2)$ for the Sierpinski carpet. For the square lattice the corresponding exponent is $\nu_\perp = 0.733(7)$.

in the Sierpinski fractal lattice versus c for several lattice sizes (different k generation). The results are reported in figure 6. The increasing peaks signal the diverging fluctuations at the critical point as the thermodynamical limit is approached. The data for the order parameter fluctuations at the critical point were used in figure 3 to obtain critical exponents ratio $\gamma'/\nu_\perp$ since $\Delta\rho(c) \propto L^{\gamma'/\nu}$ at the critical point. Our best estimate provides $\gamma'/\nu_\perp = 0.42(2)$, as seen in figure 7.

In table 1 we collect the estimated values of $\beta/\nu_\perp$, $\nu_\perp$ and $\gamma'/\nu_\perp$ for the absorbing-state transition exhibited by the present predator-prey model in the Sierpinski fractal lattice. The values for the two dimensional contact process (CP-2D) are also shown for comparison. For the square lattice the exponents are those of the directed percolation universality class in the corresponding lattice [1, 23]. Values for the CP in the
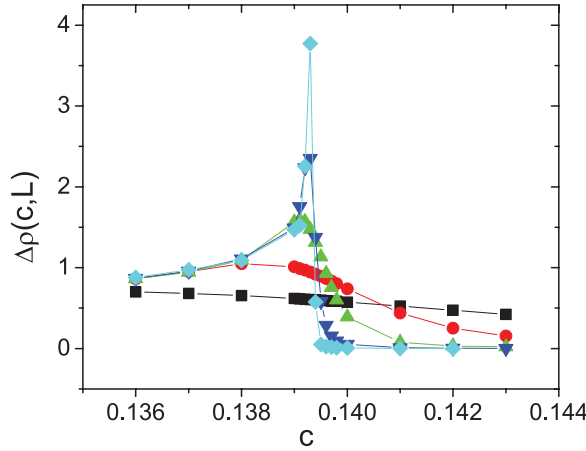
Figure 6. Order parameter fluctuations $\Delta\rho(c,L)$ versus c for distinct k generations (same values of k as in figure 2). The peak in the vicinity of the critical density signalizes the enhancement of the order parameter fluctuations near the second-order absorbing state phase transition.

Table 1. Estimated values of the stationary critical exponents $\beta/\nu_\perp$, $\nu_\perp$ and $\gamma'/\nu_\perp$ for the present predator-prey model in the Sierpinski Carpet (SC).

	$\beta/\nu_\perp$	$\nu_\perp$	$\gamma'/\nu_\perp$
Present model in the SC	0.72(3)	0.79(2)	0.42(3)
Present model in 2D	0.79(2)	0.73(1)	0.42(1)
CP in the SC	0.726(8)	0.78(1)	0.42(2)
CP in 2D	0.796(12)	0.7333(75)	0.409(24)

Note: For comparison, we also present the corresponding values for this model in 2D [1], the contact process (CP) in the Sierpinski Carpet [27], and the CP in 2D [32, 36].

Sierpinski Carpet were taken from [27]. The exponent governing the finite-size scaling of the order parameter fluctuations is only slightly affected by the lattice fractality (difference is within the error bar). On the other hand, the order parameter and correlation length exponents are quite distinct. While the correlation length exponent $\nu_\perp$ is approximately 8% larger in the Sierpinski fractal, the order parameter exponent β is 16% smaller. These exponents are similar to those of the usual contact process in the Sierpinski carpet [27]. Our estimated value for $\beta/\nu_\perp$ and $\gamma'/\nu_\perp$ leads to the hyper-scaling relation $2\beta/\nu_\perp + \gamma'/\nu_\perp = d_{\mathrm{f}} = 1.86(9)$. This value is compatible with the hyper-scaling relation $2\beta/\nu_\perp + \gamma'/\nu_\perp = d_{\mathrm{ef}} = d_{\mathrm{f}} = 1.893...$ for the Sierpinski carpet. However, the small deviation, although being within our error bars, cannot rule out a possible difference between the effective hyper-scaling dimension and the fractal dimension, as reported previously to occur in the Ising model [31].

In order to probe the dynamical critical behavior, we followed the relaxation dynamics towards the statistically stationary state. It is important to stress that the critical dynamics for the survival of a single active particle, an individual predator in the present model, is quite non-trivial in heterogenoeus media [34, 35]. For the usual contact process in a randomly diluted square lattice, the critical spreading was shown to be logarithmic with a Griffiths phase below the critical point with non-universal power-laws [34]. Further, it has been shown that even in the presence of a single defect, the
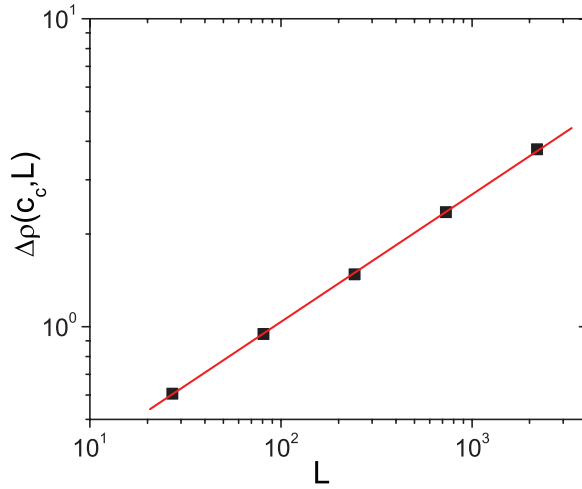
Figure 7. Log–log plot of the order parameter fluctuations $\Delta\rho(c_c, L)$ versus L at the critical point. The exponent ratio $\gamma'/\nu_\perp$ is estimated from the slope of the fitted straight line providing $\gamma'/\nu_\perp = 0.42(3)$. For the square lattice, the corresponding value is $\gamma'/\nu_\perp = 0.42(1)$.

critical spreading of active particles starting from the defect site acquires a strecthed exponential form [35]. Here, we will probe just the critical relaxation of a well developed active state, starting from an initial condition with half of the allowed sites occupied by predators while the other half is occupied by prey. The time evolution of the order parameter, its moment ratio and fluctuations can be used to estimate some dynamical critical exponents. In what follows, we considered the relaxation process in chains with $L = 6561$ sites ($k = 8$) and averaged the quantities over $n = 200$ distinct runs. Calculations were performed up to $t = 10^5$ MCS.

The order parameter density relaxes towards its stationary value following the dynamic scaling law $\rho(c_c, t) \propto t^{-\beta/Z\nu_\perp}$ where $Z = \nu_\parallel/\nu_\perp$. In figure 8 we show such time evolution for $k = 8$ and three distinct death rates close to the critical point. In figure 9 we present an independent calculation of the critical transition point by the standard deviation and correlation coefficient method. We found that this method leads to $c_c = 0.139\,34(1)$, with the value of the standard deviation in a minimum while the correlation coefficient presents a maximum signalizing the transition. The value for c_c is consistent (within error bars) to the one obtained from the statistically stationary cumulant technique. The power-law relaxation of the order parameter provides the estimate $\beta/Z\nu_\perp = 0.39(2)$.

The dynamic scaling hypothesis also predicts that the moment ratio $U_L(c_c, t) \propto t^{d_f/Z}$. In figure 10 we report such relaxation of the order parameter moment ratio. The estimated value of the dynamic exponent $Z = 1.88(5)$ is also included in table 2. This value is larger than the critical exponent in the square lattice reflecting the slower critical relaxation dynamics taking place in the fractal environment. The above dynamical exponents can be used to obtain an independent estimate of the stationary exponent ratio $\beta/\nu_\perp$ which is also consistent with the value reported in table 1 within the error bars.

The time evolution of the order parameter fluctuations is shown in figure 11. Dynamical scaling predicts $\Delta\rho(c_c, t) \propto t^{\gamma'/Z\nu_\perp}$. The estimated critical exponent $\gamma'/Z\nu_\perp = 0.21(3)$ is
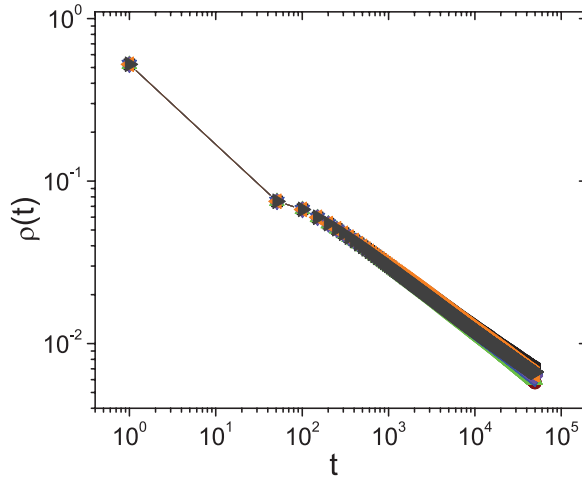
Figure 8. Time evolution of the order parameter at the critical point for a generation $k = 8$ ($L = 6561$) and several death rates c in the vicinity of the critical point. Data are averages over 200 distinct runs. The dynamic scaling law $\rho(c_c, t) \propto t^{-\beta/z\nu_\perp}$ holds after a short transient. The estimate of this critical exponent ratio is reported in table 1.
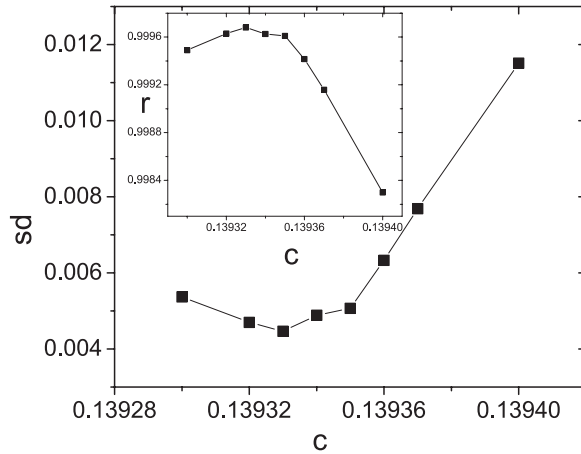

Figure 9. Independent determination of the critical point by exploring the short-time dynamics for $k = 8$. Standard deviation and correlation coefficients are measured relative to the best power-law fitting of the numerical data. We have found $c_c = 0.139\,34(1)$ at the critical point which provides maximum correlation and minimum deviation.

also reported in table 2. Combined with the above estimate of Z, this value provides an estimate of $\gamma'/\nu_\perp$ compatible with the one provided by the stationary state analysis within the error bars. Finally in figure 12 we present the result of the exponent $\nu_\|$ calculated from the dynamic scaling relation:

$$\frac{\mathrm{d} \log \rho(c \approx c_c, t)}{\mathrm{d}c} \propto t^{1/\nu_\|}. \tag{5}$$

The estimated value $\nu_| = 1.51(2)$ is also consistent with the former estimated exponents Z and $\nu_\perp$.
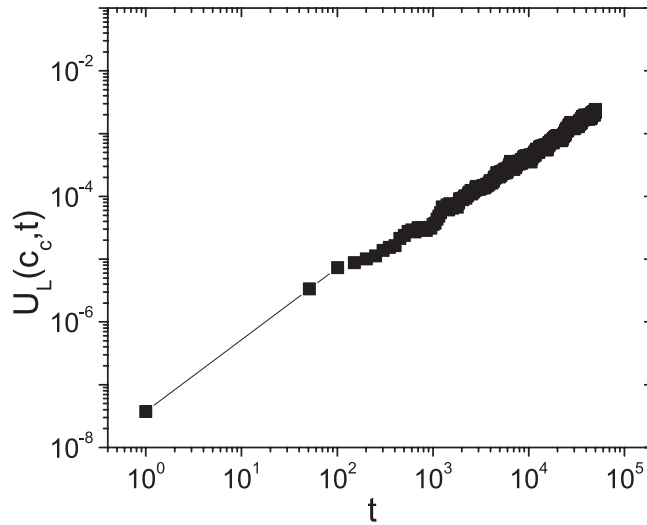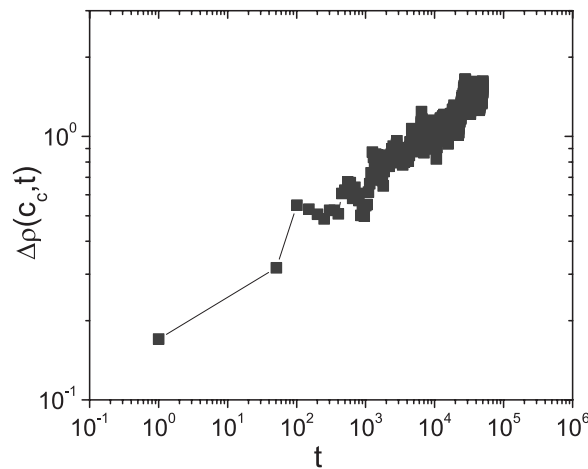
Figure 10. Time-evolution of the order parameter moment ratio at criticality. Same conditions as in figure 8. The dynamic scaling law $U_L(c_c, t) \propto t^{d_f/Z}$ holds in the short-time regime. Using $d_f = \ln 8/\ln 3$, we estimated the dynamic exponent Z (see table 2).

Table 2. Estimated values of dynamical critical exponents $\beta/Z\nu_\perp$, Z, $\gamma'/Z\nu_\perp$ and $\nu_\parallel$ for the present predator-prey model in the Sierpinski Carpet (SC).

	$\beta/Z\nu_\perp$	Z	$\gamma'/Z\nu_\perp$	$\nu_\parallel$
Present model in the SC	0.39(2)	1.88(5)	0.21(3)	1.51(2)
Present model in 2D	0.451(6)	1.763(6)	—	1.29(10)
CP in the SC	0.39(1)	1.88(5)	0.24(2)	1.49(3)
CP in 2D	0.4505(10)	1.7660(16)	0.231(14)	1.2950(60)

Note: For comparison, we also present the corresponding values for this model in 2D [23], the contact process (CP) in the Sierpinski Carpet [27] and the CP in 2D [32, 36].

Figure 11. Time evolution of the order parameter fluctuations at criticality. Same conditions as in figure 8. The dynamic scaling law $\Delta\rho(c_c, t) \propto t^{\gamma'/Z\nu_\perp}$ holds in the short-time regime. Our estimate of this critical exponent ratio is reported in table 2.
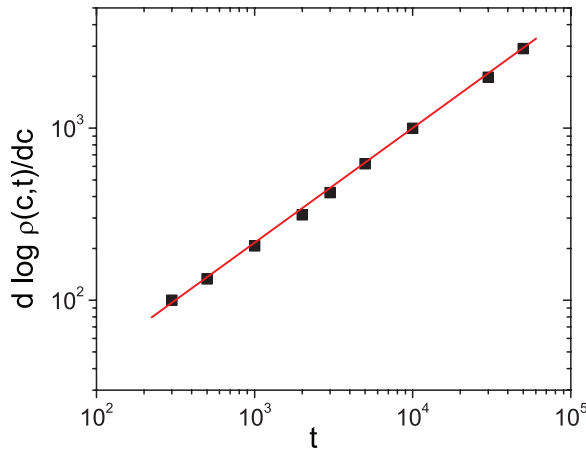
Figure 12. Log–log plot of the derivative of $\ln \rho(c, t)$ at the critical point. Same conditions as in figure 8. The dynamic scaling law $\mathrm{d}\ln\rho(c, t)/\mathrm{d}c\big|_{c_c} \propto t^{1/Z\nu_\perp}$ holds in the short-time regime. We estimated $\nu_\parallel = 1.51(2)$ (see table 2).

4. Summary and conclusions

In summary, we investigated the influence of landscape fractality on the absorbing-state phase transition taking place in a stochastic predator-prey population dynamics model. The main control parameter was taken as the death rate of predators which is inversely proportional to predators average lifetime. For small death rates the system evolves towards a statistically stationary state with coexisting predator and prey populations. Above a critical death rate the predators become extinct. As a prototype fractal landscape we considered the Sierpinski carpet which has fractal dimension $d_\mathrm{f} = \ln 8\,/\,\ln 3 = 1.89$ just slightly below the dimension of an Euclidean surface $d = 2$. We showed, however, that fractality has a relatively large impact on the survival of the predator species, promoting a significant reduction in the critical death rate driven by the substantial decrease of the average local connectivity. As a consequence, the evolution pressure driven by the natural selecting principle in fractal landscapes shall favor the survival of predator species with larger lifetimes.

In fractal lattices intrinsic topological properties other than dimensionality may alter the critical behavior of equilibrium systems. In non-equilibrium phase transitions, the dynamic evolution couples with the scale-invariant topology, which may result in the emergence of an unconventional critical behavior [27]. The landscape fractality also impacts on the universal critical behavior of the absorbing state transition. However, the characteristic finite-size scaling exponents in the vicinity of the absorbing transition are not affected uniformly. While those related to the population density fluctuations are barely affected, those associated with the population density and the correlation length and time scales depict measurable deviations from the usual 2D behavior. All exponents reported are consistent with the transition belonging to the directed percolation universality class presented by the usual contact process model in the same fractal landscape.

Acknowledgments

References

[1] Argolo C, Otaviano H, Gleria I, Arashiro E and Tomé T 2010 *Int. J. Bifurcation Chaos* **20** 309
[2] Tainaka K 1989 *Phys. Rev. Lett.* **63** 2688
[3] Durret R and Levin S 1994 *Theor. Popul. Biol.* **46** 363
[4] Satulovsky J E and Tomé T 1994 *Phys. Rev.* E **49** 5073
[5] Boccara N, Roblin O and Roger M 1994 *Phys. Rev.* E **50** 4531
[6] Provata A, Nicolis G and Baras F 1999 *J. Chem. Phys.* **110** 8361
[7] Antal T and Droz M 2001 *Phys. Rev.* E **63** 056119
[8] Antal T, Droz M, Lipowsky A and Odor G 2001 *Phys. Rev.* E **64** 036118
[9] Ovaskainen O, Sato K, Bascompe J and Hanski I 2002 *J. Theor. Biol.* **215** 95
[10] de Aguiar M A M, Rauch E M and Bar-Yam Y 2003 *Phys. Rev.* E **67** 047102
[11] de Carvalho K C and Tomé T 2004 *Mod. Phys. Lett.* B **18** 873
[12] Szabó G and Sznaider G A 2004 *Phys. Rev.* E **69** 031911
[13] Mobilia M, Georgiev I T and Tauber U C 2006 *Phys. Rev.* E **73** 040903
[14] de Carvalho K C and Tomé T 2006 *Int. J. Mod. Phys.* C **17** 1647
[15] Hill M F and Caswell H 1999 *Ecol. Lett.* **2** 121
[16] Imre A R and Bogaert J 2004 *Acta Biotheor.* **52** 41
[17] Bell S S, Mccoy E D and Mushinski H R (ed) 2012 *Habitat Structure: the Physical Arrangment of Objects in Space* (Berlin: Springer)
[18] Arashiro E, Rodrigues A L, de Oliveira M J and Tomé T 2008 *Phys. Rev.* E **77** 061909
[19] Rodrigues A L and Tomé T 2008 *Braz. J. Phys.* **38** 87
[20] Nisbet R M and Gurney W S C 1982 *Modeling Fluctuating Populations* (New York: Wiley)
[21] Tomé T and de Oliveira M J 2009 *Phys. Rev.* E **79** 061128
[22] Tomé T and de Oliveira M J 2015 *Stochastic Dynamics and Irreversibility* (New York: Springer)
[23] Arashiro E and Tomé T 2007 *J. Phys. A: Math. Theor.* **40** 887
[24] Fried Y, Ben-Zion Y and Shnerb N M 2013 *New J. Phys.* **15** 113018
[25] Huffaker C B 1958 *Hilgardia* **27** 343
[26] Milne B T 1992 *Am. Nat.* **139** 32
[27] Argolo C, Barros P, Tomé T, Gleria I and Lyra M L 2015 *Phys. Rev.* E **91** 052137
[28] Fulco U L, Messias D N and Lyra M L 2001 *Phys. Rev.* E **63** 066118
[29] Dickman R, Tomé T and de Oliveira M J 2002 *Phys. Rev.* E **66** 016111
[30] Tomé T and de Oliveira M J 2005 *Phys. Rev.* E **72** 026130
[31] Bab M A, Fabricius G and Albano E V 2005 *Phys. Rev.* E **71** 036139
[32] Lubeck S and Willmann R D 2005 *Nucl. Phys.* B **718** 341
[33] Carmona J M, Marconi U M N, Ruiz-Lorenzo J J, Tarancón A 1998 *Phys. Rev.* B **58** 21
[34] Moreira A G and Dickman R 1996 *Phys. Rev.* E **54** R3090
[35] Barato A C and Hinrichsen H 2011 *J. Stat. Mech.* P02035
[36] Henkel M, Hinrichsen H and Lubeck S 2008 *Non-Equilibrium Phase Transitions: Absorbing Phase Transitions* vol I (Berlin: Springer)